# Stony Brook University

**Study of Polyamide Barrier Layers in Reverse Osmosis Membranes**

A Thesis Presented

by

**Qinyi Fu**

to

The Graduate School

in Partial Fulfillment of theRequirements

for the Degree of

**Master of Science**

in

**Chemistry**

Stony Brook University

**August 2017**

**Stony Brook University**
The Graduate School

**Qinyi Fu**

We, the thesis committee for the above candidate for the
Master of Science degree, hereby recommend
acceptance of this thesis.

**Benjamin S. Hsiao – Thesis Advisor**

**Distinguished Professor, Department of Chemistry**

**Ken A. Dill– Chairperson of Defense**

**Distinguished Professor, Department of Chemistry**

**Esther S. Takeuchi– Third Member**

**Distinguished Professor, Department of Chemistry, Department of Materials Science and Chemical Engineering**

This thesis is accepted by the Graduate School

Charles Taber
Dean of the Graduate School

Abstract of the Thesis

**Study of Polyamide Barrier Layers in Reverse Osmosis Membranes**

by

**Qinyi Fu**

**Master of Science**

in

**Chemistry**

Stony Brook University

**2017**

Fresh water scarcity is an urgent challenge in many regions around the world, where desalination of brackish water and seawater has become one of the most promising solutions. In desalination, the reverse osmosis (RO) membrane technology, developed in 1960s, is the most state-of-the art solution. However, the relatively low filtration efficiency of RO membranes is still the major hurdle that limits the overall performance of desalination. Currently, interfacial polymerization is a common approach to fabricate RO membranes, in which two reactive monomers: such as m-phenyldiamine (MPD) and Tirmesoyl chloride (TMC), dissolved in two immiscible phases (i.e., aqueous and organic phases, respectively), can react at the interface to form a thin polyamide barrier layer. To overcome the low filtration efficiency (low flux), it is important to learn the formation mechanism of polyamide layer and the resulting structure. For this purpose, we first investigated the freestanding polyamide layer without the scaffold support. In specific, grazing-incidence wide-angle X-ray scattering (GIWAXS) was used to inspect the inter-molecular structure of free-standing polyamide layer, with the layer thickness was controlled at around 3 nm, where reflectometer was used to determine the film thickness and

surface smoothness. The results revealed the relationships between the barrier layer thickness, monomer concentrations, monomer types during interfacial polymerization. Finally, the RO membrane based on the same polyamide barrier layer was tested by a high-pressure desalination system at 800 psi, to correlate the polyamide structure with desalination performance.

## Table of Contents

**Acknowledgement**

First, I would like to thank Electric Power Research Institute (EPRI- 77846) for the financial support of my research.

Second, I would like to express my heartfelt gratitude to Prof. Benjamin Hsiao, Prof. Benjamin Ocko and Prof. Hongyang Ma for their helpful advice, generous support and endless encouragement. I would also like to thank my committee members: Prof. Ken Dill and Prof. Kenneth Takeuchi for their valuable comments and suggestions.

Finally, my thanks go to my colleagues: Kai Liu and Xiangyu Huang for helping me to prepare freestanding samples, Andre Yin and Coby Yeung for helping me with the desalination test.

# Chapter 1. **Introduction**

## 1.1. **Reverse osmosis technology overview**

The reverse osmosis (RO) thin-film composite (TFC) membrane was first developed in 1965[1][2] to desalinate seawater. Since then, the TFC membrane technology has experienced astounding growth through the research of optimizing reaction conditions[3], introducing nanoparticles[4] and effective additives such as surfactants[5]. The fabricating method to produce the surface barrier layer in TFC membranes is through the process of interfacial polymerization (IP), where two monomers dissolved in two immiscible solvent can react and form an ultra-thin polyamide layers on a porous substrate[6]–[8]. This ultra-thin layer is responsible for filtering out hydrated salt ions with size less than 1 nm. However, little has been known as how this dense-core layer forms and what is the structure and reaction relationship in this layer[9], [10].

## 1.2. **Interfacial polymerization**

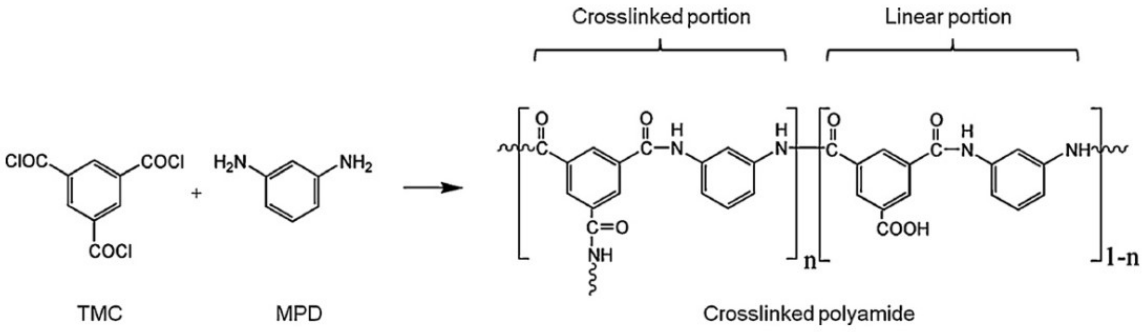


Figure 1 Schematics of interfacial polymerization

In typical RO membranes for seawater desalination, the aromatic polyamide layer formed by interfacial polymerization involves two reactive monomers: m-phenylenediamine (MPD) and

trimesoyl chloride (TMC), where reaction takes place on the surface of a microporous support[11]. Figure 1 shows the schematic chemical reaction diagram of interfacial polymerization, where the resulting structure consists of a partially crosslinked network[12], [13]. During the interfacial polymerization reaction, MPD passes through a porous support and react with TMC. Because TMC in immiscible in water, the reaction is limited to the substrate surface. In the interfacial polymerization experiment, efforts were made to make polyamide layer well attached to the substrate to prevent leaking. And polyamide layer is robust and can withstand 800 psi of desalination pressure. However, little has been known about the in-depth mechanism of forming this dense-core layer.

### 1.3. Concentration effect on polyamide layer morphology

In a recent paper, the authors used a sacrificial layer on porous substrate under polyamide layer. They achieved 8 nm polyamide ultra-thin layer[14] and separated it on a silicon wafer for

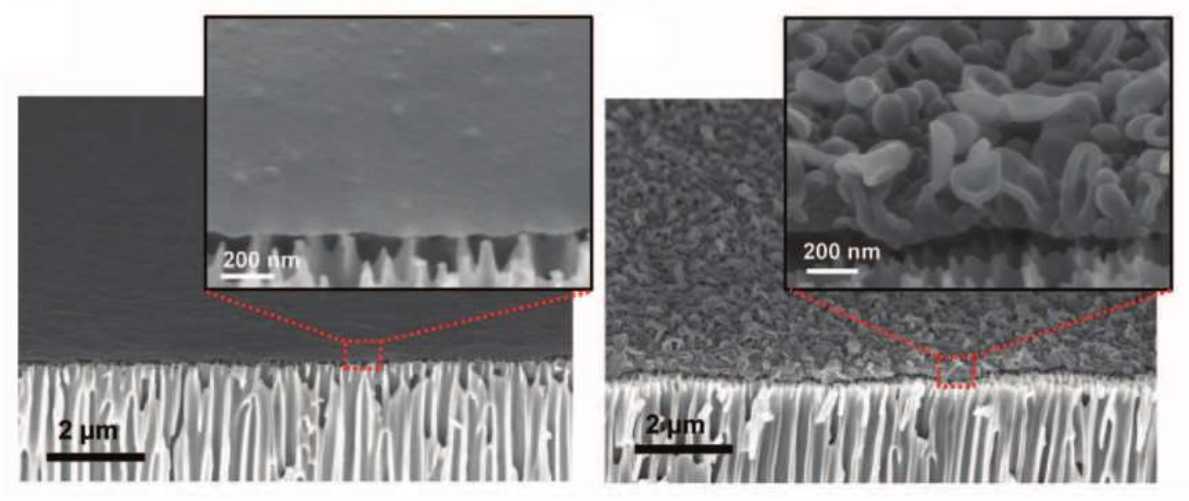


Figure 2 Comparison of polyamide morphologies composed of different MPD/TMC concentration. Left: smooth nanofilm (MPD 0.1wt%, TMC 0.005wt%, reacted for 10min); Right: crumpled nanofilm (MPD 3 wt%, TMC 0.15 wt%, reacted for 1min)

the characterization with SEM.

Figure 2 shows the schematic of interfacial polymerization on PES substrate and its SEM image of the cross-sectional view and top view. It was interesting to note that different concentrations of monomers create different surface morphology of the polyamide layer, where a smooth surface has been achieved from low concentration of monomers, and high concentration, however, issued crumpled surface to the membrane. It was explained that an interfacial polymerization is diffusion controlled and self-limiting, as a result, once the film is formed, it is so dense that the monomers cannot pass through anymore. Therefore, the free monomers have to diffuse to the other side before the layer formed, and they likely to react with near branches, and therefore make the long branches of polyamide have a competing advantage. Unfortunately, there are limited studies focus on the structure formation of the polyamide layer by interfacial polymerization, and the corresponding mechanism is unclear yet.

### 1.4. **X-ray studies conducted on polyamide layer**

X-ray scattering is a powerful method to probe into molecular scale structure of polymer films. However, only few papers have conducted small angle scattering (SAXS) or wide angle scattering (WAXS) research on polyamide layer of reverse osmosis membrane[15], [16]. A series of bulk polyamide samples made at the organic-water interface with different TMC concentrations, and the X-ray scattering graphs were shown in Figure 3.

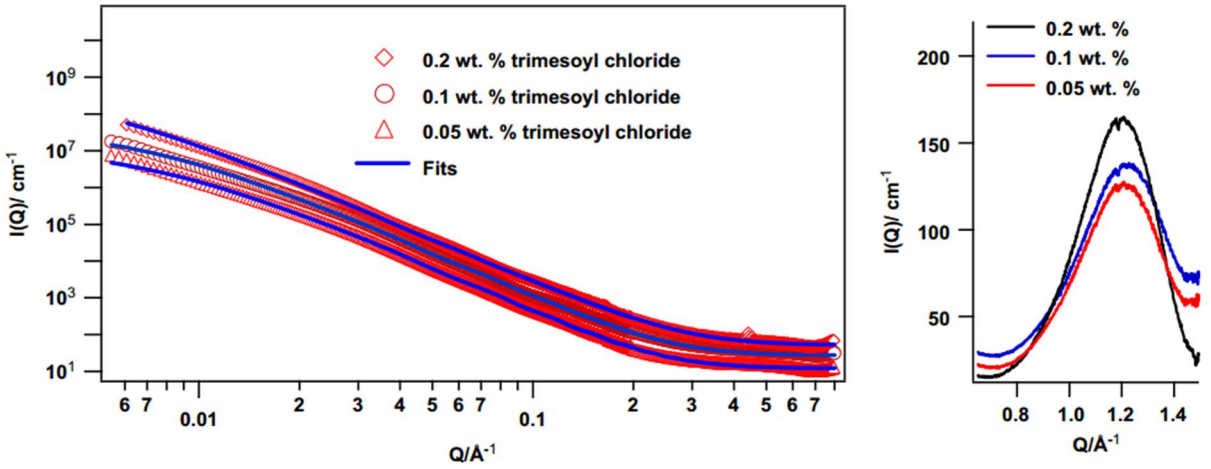


Figure 3 Small angle (left) and wide angle scattering (right) of different TMC concentrations (0.2 wt%, 0.1 wt%, 0.05 wt%), MPD 2.0 wt%. For small angle data, excellent fits were achieved using model of mass fractal cluster-like structure formed by globular unit in SASfit program. For wide angle data, the peak reveals the average molecular spacing given by $M_p = \frac{2\pi}{Qz}$.

For small angle profile, the overall equation is given by

$$I(Q) = \phi \Delta\rho^2 V F(Q) S(Q)$$

where $\phi$ is the particle number density of scattering particle, $V$ is the volume, $\Delta\rho^2$ I the contrast factor, $F(Q)$ is the form factor, and $S(Q)$ is particle distribution. In this paper, Singh uses spherical form factor $F(Q)$

$$F(Q) = \left[3\frac{(\sin(QR) - QRcos(QR)}{(QR)^3}\right]^2$$

And $S(Q)$ is described as [13], [17], [18]

$$S(Q) = 1 + 4\pi\bar{N}\int_0^\infty dr\, r^2[g(r) - 1]\frac{\sin(Qr)}{Qr}$$

where $g$ is the pair correlation function. This model is namely mass fractal cluster-like structure formed by globular unit. It gives perfect fitting for SAXS data as shown in Figure 3[13], [19] on the left.

For wide-angle X-ray scattering, it reveals more information about primary structural unit. The authors observed a wide peak between $Qz = (0.8,1.4)$. This peak reveals average molecular spacing, which is estimated to be 5.2-5.3 Å.

A comparing study on SAXS and WAXS measurements of polyamide film was conducted [15] where a loose polyamide film fabricated by using 20 g/L MPD and 1g/L TMC exhibited both 10 times larger than the results from ref [xx]. The average molecular spacing peak of loose polyamide located at 1.34 $Å^{-1}$ compared with 1.21 $Å^{-1}$ reported from dense polyamide filmTherefore, the average molecular spacing is 4.7 Å rather than 5.2 Å. Also, the comparison has been made between GIWAXS data of the film polyamide on polysulfone with that of polysulfone GIWAXS, a peak at 1.31 $Å^{-1}$ is observed which can be attributed to $\pi$-stacking of conjugated polymers. Encouraging by this study, adetailed structure model for polyamide layer should be established and how do the monomer concentrations affect on polyamide layer should be explored.

### 1.5. **Simulation studies conducted on polyamide layer formation**

A simulation was done by Honig et al[20] who used cluster-cluster aggregation algorithm to simulate interfacial polymerization process. CCA (define!) model considers cluster movement and its mobility is proportional to cluster size[21]. Particles aggregation upon contact and

continuously grows larger. This model is an established model to explain porous structures of a polymer film [22], [23].

The film formation process in great details can be described as follows: Assuming that a trial move calculated above is accepted, and there are two monomers in contact with at least one functional groups, then, two monomers are bonded with a possibility of $\mathrm{p}_{i,\alpha}^{\beta}$. The simulation will proceed to $2\times10^7$ cycles till the reaction rate close to zero.

The probability $\mathrm{p}_{i,\alpha}^{\beta}$ is calculated as

$$\mathrm{p}_{i,\alpha}^{\beta} = \sum_{\varphi=\alpha,\beta} K_i^{\varphi} f_i$$

where $\mathrm{p}_{i,\alpha}^{\beta}$ is the ratio of reaction for particle $i$ for solvent type $\alpha$ to environment $\beta$. $K_i^{\varphi}$ is the partition coefficient of particle $i$ in solvent $\varphi$, and $f_i$ is the fraction of particles of type $i$ in local environment.

Time scaling is done by comparing the actual diffusivity with calculated diffusivity in the solution[22], [23], where the estimated film thickness was about 5 nm.

$$< D >= \frac{\sum_{i=1}^{n} {\Delta r_i}^2}{6n\Delta t}$$

Where n is particle number, $\Delta r_i$ is the displacement of particle $i$ in time $\Delta t$.

.

In reality, however, TMC monomers in organic phase cannot diffuse into aqueous solution, as a result, the polyamide film can forms only at organic phase. Also, it still cannot explain why the

crumpled polyamide surface with branches at high concentration can be formed. There are some simulation works focus on the factors that affect polyamide layer thickness[24], [25].

## 1.6. **Research overview**

My research aims to address the following questions:

1. How does an interfacial polymerization process form a polyamide layer with designed dense core structure?
2. What is the correlation between the polyamide structure and water molecules diffusion during a desalination process?

X-ray study of freestanding polyamide layer structure may provide some new insights into these two questions. My research activities included:

1. Freestanding polyamide layer at the liquid-liquid interface instead of on the surface of a porous substrate was prepared to simplify structure characterization. Also, ultra-thin layer (3.3nm) with few polyamide molecular layer was made.
2. Reflectometry was used to measure the thickness and roughness of polyamide layers.
3. Grazing incidence X-ray scattering was used to probe into intra-molecular structures of polyamide layer. Samples made by different concentrations, monomer types and on-substrate layer were also tested and compared.
4. Desalination tests were conducted to correlate the polyamide layer structure with desalination performance.

# Chapter 2. **Preparation of freestanding polyamide layer**

## 2.1. **Freestanding layer preparation procedure**

The preparation procedure of freestanding polyamide layer is described as following[26]. First a silicon wafer is prewashed with solvents. The silicon wafer used in this experiment is 1×2 inch to ensure that the sample is large enough for further test. Place acetone container on a hot plate and warm up to 55 °C. Then place the silicon wafer in acetone for 10 min. Subsequently, the silicon wafer is taken out to methanol solvent for 2-5 min to remove acetone residues. Finally, the silicon wafer was rinsed with DI water for 5 times, and was blew with nitrogen gas[27]. Then the sample is ready to treat with RCA (define!) solution.

A standard RCA cleanser is made of 50mL of water, 10mL of 27% ammonium hydroxide and 10mL of hydrogen peroxide. First, ammonium hydroxide is added to 50mL of water and the solution was heated up to 70 °C. Followed, remove the solution container from the hot plate and add 10mL of hydrogen peroxide aqueous solution (concentration?). The solution will then be bubbled for 2 minfollowed by taking out the silicon wafer and rinsing it with DI water. The cleaning effects can be checked by performing a wetting test. If a water droplet can spread off on the surface, it indicates there are no oil residues on the surface of the silicon wafer. Consequently, the silicon wafer is dried with nitrogen blower and treated with an ozone cleaner for 10 min[26]. The ozone cleaner used is Compact UV-Ozone Cleaner with 4"x 4" Chamber - EQ-PCE-44-LD.

The pre-washed silicon wafer is then placed in a 50mL-beaker. Afterwards, 5mL of 0.1 wt% MPD solution is added to the beaker. By then the silicon wafer surface is just immersed into the solution. Consequently, in the subsequent draining process, the polyamide layer forms at the liquid-liquid interface could be remained and deposited directly on the silicon substrate. Then

2mL of pure hexane is added to the beaker, forms a solvent layer of 0.4 mm thickness on top of MPD solution. The thickness of this layer is a controlling parameter in the diffusion-controlled interfacial polymerization. Also, it is used as a 'cushion' to reduce the turbulence from dropping down the TMC solution, and therefore, a smooth and even film could be created. Subsequently, 1mL of 0.05 wt% TMC solution is dropped carefully on the top of the hexane layer. The droping amount was made within 2mm overtop the hexane layer surface, and evenly distributed across the surface. Then the reaction starts with the meeting of TMC monomers and MPD monomers at the interface. The estimated diffusion time for 0.4mm hexane is approximately 40 min. Therefore, the reaction time was desired as 1 h before moving to the next step.

The next step was to drain the excess solution and leave the polyamide layer on the silicon substrate. A syringe pump (model NE-1010 from syringepump.com) with a 60mL syringe was used. The syringe was connected to a ID 1/4 " PVC clear tubing, and the tubing connects to a 10ml-glass pipet. The glass pipet bottom is fixed just above the 50ml beaker bottom to ensure that all the liquid can be drained. The pipet is stabilized by a stand. This setup is prepared before to prevent any disturbance on IP reaction. The draining speed is set as 10mL/min.

Finally, a post-treatment was carried out by adding 5mL of 1 wt% of acidic acid to neutralize excessive MPD monomers. In details, 5ml of acidic acid was carefully dropped near the silicon wafer and spread slowly on the surface of the polyamide film. After 30 min, the solution was drained at 10mL/min using the same setup. Finally, the polyamide sample was kept in a desiccator at 25 °C for further use.

### 2.2. **Controlling variables on film thickness**

Interfacial polymerization is a diffusion-controlled process between two phases. Therefore, the film formation correlated with the monomer types, monomer concentrations, and solvent [28]. The experiments based on this consideration are designed as follows.

1) Monomer type

Monomers in the aqueous phase: m-phenylenediamine (MPD) and piperazine (PIP)

In the previous studies, a polyamide membrane fabricated from PIP and TMC monomers was used for nanofiltration, while polyamide based on MPD monomer was used for reverse osmosis. The comparison between these two monomers could reveal the relationship of average molecular spacing versus filtration target size.

2) Concentration

Monomer concentration is one of key points for interfacial polymerization. As in previosu study, a transformation of a polyamide layer from smooth and even (MPD 0.1 wt% TMC 0.005 wt%, reaction time 10 minutes) to crumpled and uneven (MPD 3 wt% TMC 0.15 wt%, reaction time 1 minute) can be observed. Meanwhile, an ultra-thin layer (3.3 nm) was formed by using ultra low concentration of monomers.

The experimental conditions were depicted as follows:

1. MPD concentration variation

| | | | | |
|---|---|---|---|---|
| TMC wt% | 0.005 | 0.005 | 0.005 | 0.005 |
| MPD wt% | 0.1 | 0.01 | 0.001 | 0.0001 |

2. TMC concentration variation

| | | | | |
|---|---|---|---|---|
| TMC wt% | 0.5 | 0.05 | 0.005 | 0.0005 |
| MPD wt% | 0.1 | 0.1 | 0.1 | 0.1 |

3. Both monomers' concentration variation

| | | | | |
|---|---|---|---|---|
| TMC wt% | 0.0005 | 0.005 | 0.05 | 0.5 |
| MPD wt% | 0.001 | 0.01 | 0.1 | 1 |

3) Preparation of polyamide layer on polysulfone substrate

A polysulfone ultrafiltration membrane was used as the support for in the fabrication of reverse osmosis membrane. Previous studies have used on-substrate polyamide layer to conduct SAXS and WAXS study. Therefore, it is necessary to prepare on-substrate samples in our experiments.

The preparation procedure is described as follows. The full procedure should be carried out in dark due to the sensitive of MPD to light. First a 6×6 inch polysulfone membrane was immersed in 2 wt% MPD solution for 2 min. After the membrane was saturated with MPD solution, it was transfered on an glass plate of 8×8-inch size with 1/8 inch thickness. A glass rod was used to remove excess MPD solution from the substrate. Then the 4 edges of the substrate was taped to the glass plate using an Ultra-Adhering 3M Scotch Packaging Tape. Afterwards, the glass plate was tilted at 30 ° angle and 10 mL of 0.1 wt% hexane solution was evenly delivered on the surface of the substrate. The membrane surface was dried for 1 min, followed by put in an oven at 90 °C for 20 min. The RO membrane is then ready to be used.

The concentration variation for polyamide film on polysulfone is set as below.

| | | | |
|---|---|---|---|
| TMC wt% | 0.05 | 0.1 | 3 |
| MPD wt% | 1 | 2 | 10 |

# Chapter 3. **Reflectometry test**

Reflectometry is a technique that measures the polarization of the scattered light from multiple interfaces from a matter of multiple layers, and therefore determines the electron density and thickness of each layer of the matter[29], [30]. Reflectometry is feasible in that it does not require additional parameters to determine layer thickness, and therefore to simplify the measuring results. Furthermore, the fitting calculation for the result curve is rapid and straightforward, with a simple master formula that is universally applied.

Moreover, reflectometry measurement could be used to characterize the uniformity of freestanding polyamide samples before running GIWAXS test. Uniform layers show nice oscillation at $Q_Z$ range 0.00 to 0.30, however, signal from samples with uneven or even broken polyamide layer will decay fast. Also, thickness comparison of polyamide layer in various conditions can be expected to achieve some interesting results.

## 3.1. **Previous study on polyamide layer thickness**

Previous study has been conducted on polyamide on-substrate film, but none of them used reflectometry. In a paper by Ghosh et al[31], the authors measured polyamide layer thickness from TEM cross-section images. They measured polyamide thickness to understand the diffusivity effect of TMC in various solvents on film thickness. The authors compared MPD-TMC reaction in different organic phase (hexane, heptane, cyclohexane, isopar) where MPD has different diffusivity. Results showed higher diffusivity lead to apparently thicker films (350nm compared to 100 nm). They discovered that MPD diffusivity governs water permeability of MPD-TMC film and found out the effects of cross-linking on salt rejection of the membrane.

## 3.2. **Reflectometry principle and calculation**

For surface scattering, the master equation is [32]–[34]

$$\frac{R(Q_z)}{R_F(Q_z)} = \frac{1}{\rho_\infty}\left|\int_{-\infty}^{\infty} \frac{d\langle\rho_z\rangle}{dz} e^{iQ_z z}\, dz\right|^2 \quad (1)$$

So, the procedure to determine thickness profile is as follows. First, measure $R(Q_z)$ for a matter. Then divides with $R_F$ to obtain $R(Q_z)/R_F(Q_z)$. Afterwards, construct a fitting model for $\rho_z$ and calculate $\frac{R(Q_z)}{R_F(Q_z)}$ using the equation (1). Finally, fit unknown parameters such as layer thickness or electron density using the model obtained with real data.

Take step function as flat surface for an example, the reflectometry profile is calculated using equation (1).

$$\rho(z) = -H(z)$$

$$\therefore \frac{d\rho(z)}{dz} = -\delta(z) \;\; Dirac\ delta\ function$$

$$\therefore \frac{R(Q_z)}{R_F(Q_z)} = \frac{1}{\rho_\infty}\left|\int_{-\infty}^{\infty} \frac{d\langle\rho_z\rangle}{dz} e^{iQ_z z}\, dz\right|^2 = \frac{1}{1}\frac{1}{\rho_\infty}\left|\int_{-\infty}^{\infty} -\delta(z)\, e^{iQ_z z}\, dz\right| = 1$$

The density and scattering profiles were plotted in Figure 4.

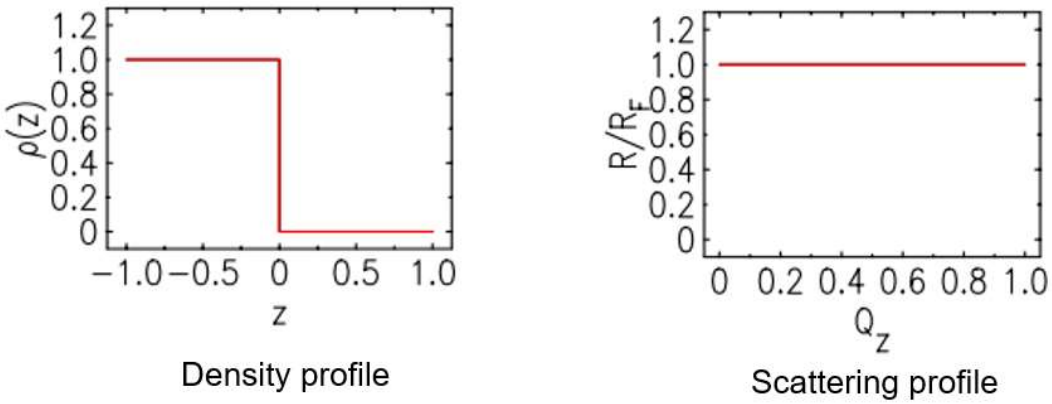


Figure 4 Reflectometry model of a flat surface

For a smeared surface, use error function

$$\rho(z) = 1 - 0.5\times erf \quad /\sqrt{2}\sigma)$$

$$\therefore \frac{d\rho(z)}{dz} = (\sigma\sqrt{2\pi})^{-1}\exp(-\sigma^2 z^2/2)$$

$$\therefore \frac{R(Q_z)}{R_F(Q_z)} = \frac{1}{\rho_\infty}\left|\int_{-\infty}^{\infty}\frac{d\langle\rho_z\rangle}{dz}e^{iQ_z z}\,dz\right|^2 = \frac{1}{1}\frac{1}{\rho_\infty}\left|\int_{-\infty}^{\infty}(\sigma\sqrt{2\pi})^{-1}\exp(-\sigma^2 z^2/2)\,e^{iQ_z z}\,dz\right|$$

$$= \exp(-\sigma^2 {Q_z}^2)$$

as shown in **Error! Reference source not found.**.

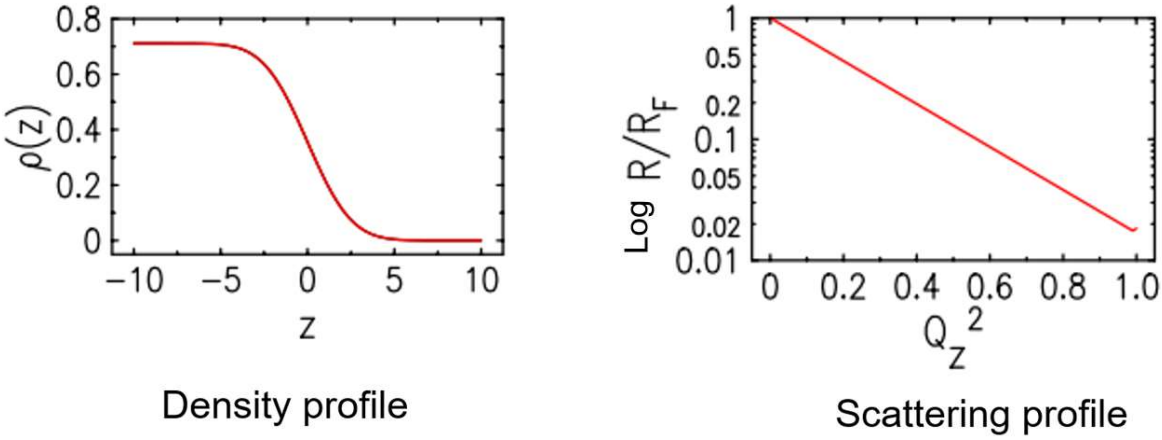


Figure 5 Reflectometry model of a smeared surface

For our samples, the film is a 3-layer matter (silicon-polyamide-air) with smeared interface, therefore the model can be described as

$$\rho(z) = \rho_0 + \frac{\rho_1 - \rho_0}{2}\,\mathrm{erf}\left(\frac{z - z_1}{\sqrt{2}\sigma_1}\right) + \frac{\rho_2 - \rho_1}{2}\,\mathrm{erf}\left(\frac{z - z_2}{\sqrt{2}\sigma_2}\right)$$

where $\rho_0, \rho_1, \rho_2$ is the electron density for silicon, polyamide and air. $z_1$ and $z_2$ is the interface position. $\sigma_1$ and $\sigma_2$ are standard deviation for interface roughness.

The error function erf(z) is written as

$$erf\left(\frac{z - z_1}{\sqrt{2}\sigma_1}\right) = \frac{1}{\sqrt{\pi}}\int_{-\infty}^{\infty} e^{\frac{(z-z_1)^2}{2{\sigma_1}^2}}\,dz$$

Use the equation (1), calculate the $\frac{R(Q_z)}{R_F(Q_z)}$ as

$$\frac{R(Q_z)}{R_F(Q_z)} = \left(\frac{\rho_1\sigma_1}{\sqrt{2}\sigma_1}e^{-\frac{1}{2}{\sigma_1}^2{Q_Z}^2}\right) + \left(\frac{\rho_2\sigma_2}{\sqrt{2}\sigma_2}e^{-\frac{1}{2}{\sigma_2}^2{Q_Z}^2}\right) + 2\frac{\rho_1\sigma_1}{\sqrt{2}\sigma_1}\frac{\rho_2\sigma_2}{\sqrt{2}\sigma_2}e^{-\frac{1}{2}({\sigma_1}^2+{\sigma_2}^2){Q_Z}^2}\cos(Q_Z\Delta L) \qquad (2)$$

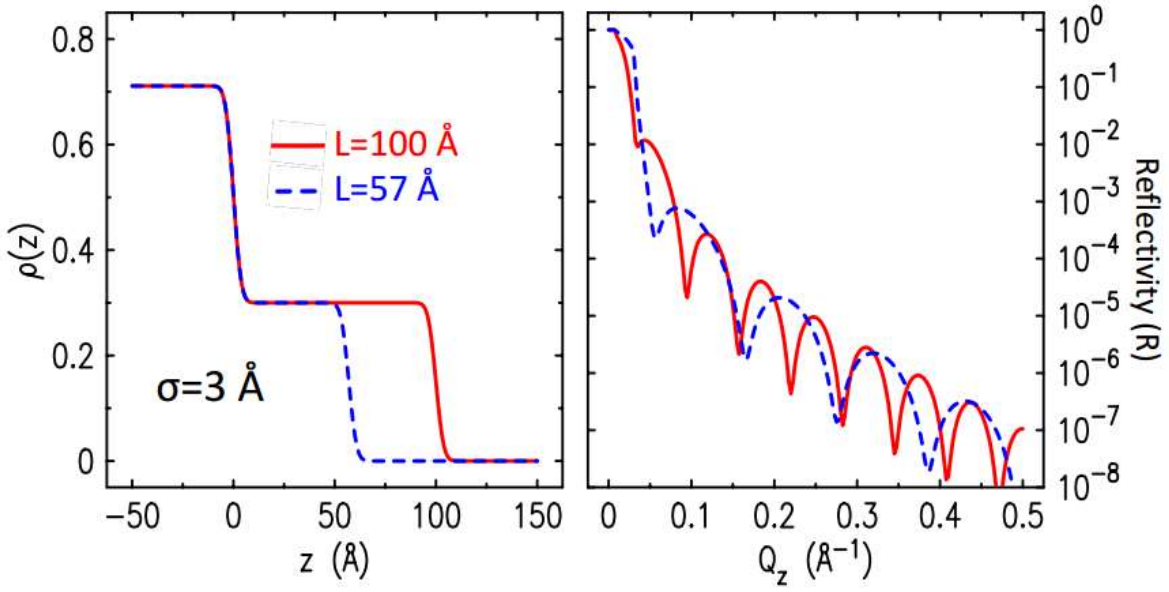


Figure 6 3-layer smeared model reflectometry profile. Left: density profile of thickness 100 Å (red line) and 57 Å (blue line). Right: reflectometry profile of two 3-layer smeared model.

The density profile is shown in Figure 6.

### 3.3. **Reflectometry testing procedure**

The reflectometry test is done on Rigaku Ultima III X-Ray Diffractometer. The x-ray wavelength is 1.54 Å, and $Q_Z$ range is set to 0.00 to 0.30. The power level for Rigaku diffractometer starts at 20keV and 2Ma, and then gradually goes up to 40 keV and 44Ma. Then click the initialization button on the software, and the machine starts going through different angles and positions.

Next step was loading a silicon wafer with freestanding polyamide layer inside the machine. The sample was loaded in the central area of the testing stage followed by hanging the slit to 5mm.

The calibration procedure is found the freestanding film position for the test. First to change the testing parameters to DivSlit=0.10 mm, SctSlit=1.00 mm, RecSlit=0.15 mm and DivH.L.Slit=10.00 mm. The incident angle is set to 0°, and the attenuator is set to 1/800. The move the z position for the testing stage from 0.5 mm to 0.7 mm. Then we get a reducing line shows the direct beam intensity change. Then find the half point of the reducing line which is estimated to be the silicon wafer surface position. Also, go over the tilting angle ($R_y$) for the testing stage and find the maximum point. Then set the sample to the pretested z and $R_y$ position. A more careful calibration is continued after changing the incident angle to 0.3°. Find the maximum point of z and $R_y$ and repeat this process for 3-4 times until the precision for z is 0.002mm, and the angle is 0.002°.

After the calibration, the measurement was start by running a preset film measurement. First to modify the position information in the file to the calibrated position above, and then to keep information about $Q_Z$ range, attenuator value and measuring time before starting running the system.

### 3.4. **Measurement results and discussion**

Fruitful results have generated from the reflectometer tests. One example is shown in Figure 7. The decay of the signal is small which shows the film is uniform. It shows a smooth and uniform film. The thickness can be estimated by $2\pi/\Delta Qz$, while $\Delta Qz$ is the oscillation period for the film. This mathematical modification is made to clearly show the oscillatory curve. The fitting result

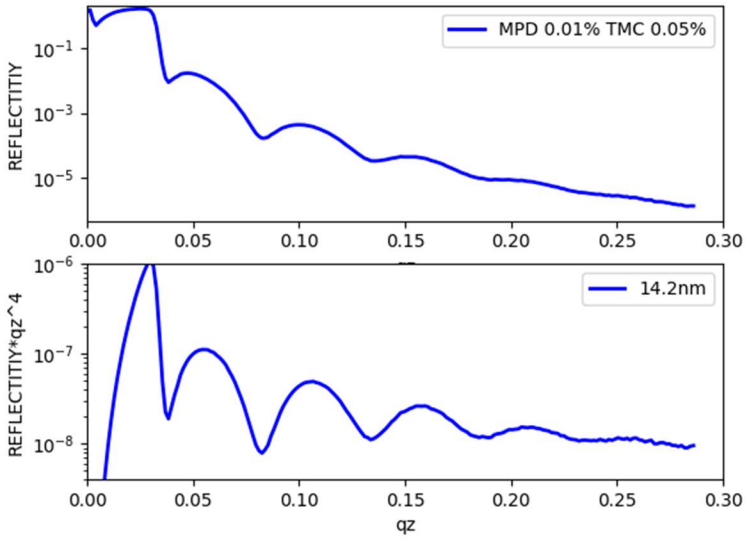


Figure 7 Reflectometer test of MPD 0.01 wt% and TMC 0.05 wt% result. Upside figure shows reflectometry data obtained from MPD 0.01 wt%, TMC 0.05 wt% solution. It shows a nice oscillation curve which indicates a smooth film. Downside figure shows reflectometry intensity times Qz to the fourth power.

for this film shows 14.2 nm.

A reflectometry fitting is applied using equation (2). The fitting result is shown in Figure 8. Three parameters were fitted: layer thickness D, layer roughness σ and layer electron density ρ. Known parameters includes silicon wafer electron density 0.7 (e/ Å3), air electron density is set to 0 (e/ Å3). The fitted electron density of polyamide is 0.38 (e/ Å3) which is close to water. For the blue line (MPD 0.01 wt% TMC 0.001 wt%), the fitting result gives thickness 33 Å and

roughness 9.4 Å. Red line (MPD 0.01 wt% TMC 0.01 wt%), is an electron density profile of higher concentration (MPD TMC). The film thickness is estimated to be 112 Å. However, the layer roughness is 8.5 Å. That means thicker film roughness is no more than thin film, which is in contrast with previously obtained SEM image. This could probably come from the difference

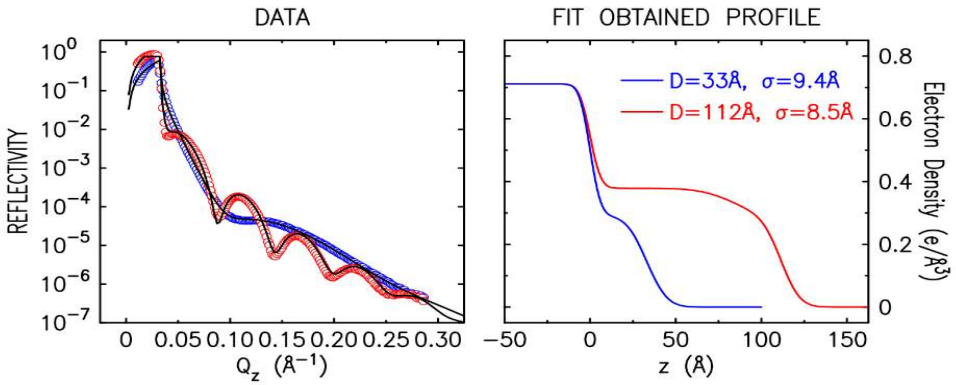


Figure 8 Fitting result for reflectometry data. Left: reflectometry data. Right: fitted electron density model. Blue line: MPD 0.01 wt% TMC 0.001 wt%, Red line: line (MPD 0.01 wt% TMC 0.01 wt%),

between freestanding film and polyamide layer grow on substrate with pores. Therefore, the diffusion through this pores will increase the roughness of polyamide film.

Figure 9 shows a reflectometry result of polyamide layers change with TMC concentration (0.001 wt%, 0.005 wt%, 0.01 wt% and 0.05 wt%). The corresponding thickness for 0.001 wt%,

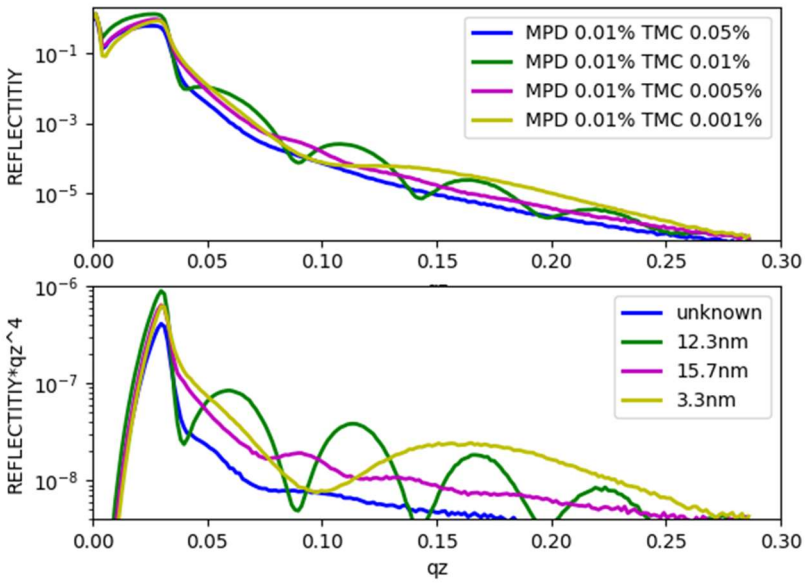


Figure 9 Reflectometry result of polyamide layers change with TMC concentration (0.001 wt%, 0.005 wt%, 0.01 wt% and 0.05 wt%), while MPD remains 0.01 wt%. Up: reflectometry data; Down: reflectometry data times Qz to the fourth power.

0.005 wt%, 0.01 wt% TMC concentration are 3.3nm, 15.7nm, 12.3nm.

Therefore, at extremely low concentration (TMC 0.001 wt%, MPD 0.01 wt%), it is possible to produce ultra-thin film of 3.3 nm which has never been reported before. However, as the concentration of TMC increase, the self-limiting factor of polyamide film growth comes to effect layer thickness, therefore, although the TMC concentration increased by 10 times from 0.005 wt% to 0.05 wt%, the film thickness remains 12-15 nm. And interestingly the thickest film obtained is from the second most diluted TMC. This possibly because the monomer concentration is low

enough, so that a quick layer could not be formed, as a result, the monomers have enough time to diffuse to the other side and then grew into a thicker film.

# Chapter 4. **GIWAXS test on freestanding polyamide layer**

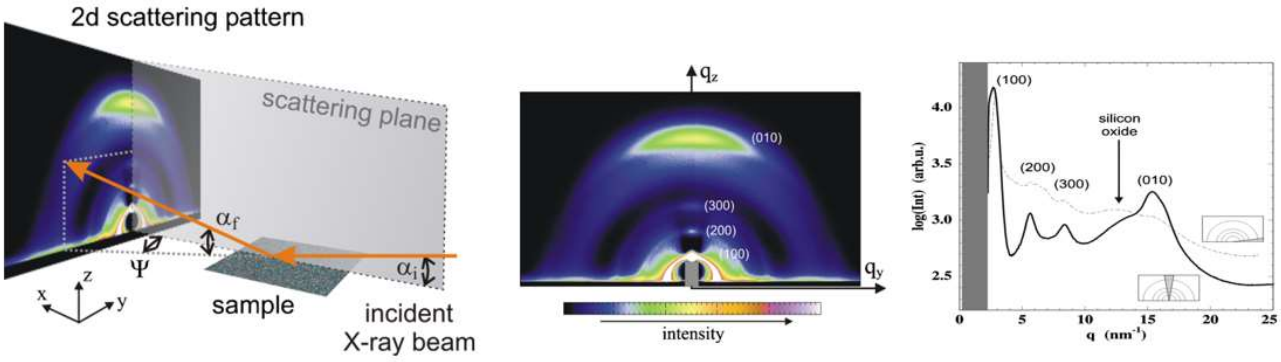


Figure 10 GIWAXS setup and data explanation. Left: GIWAXS schematic geometry; Middle: GIWAXS acquired data; Right: GIWAXS radius integrated intensity profile.

## 4.1. **GIWAXS principle and setup**

GIWAXS stands for grazing incidence wide angle scattering. It is a scattering technique used to study nanostructured surfaces and thin films[35]–[37].

The 1D scattering profile can be explained as

$$I \sim |F|^2 S$$

Where $F$ is the form factor and $S$ is the structure factor.

The form factor $F$ is given by

$$F = \int \rho(r) e^{iQr} dr$$

Where $\rho(r)$ is the electron density, $Q$ is the scattering vector, r is the scattering point position vector.

The structural factor $S$ for sphere is given by Percus-Yevick approximation[38].

$$S(q) = \frac{1}{1 + 24\eta G(2QR)/2QR}$$

Where $\eta$ is the volume fraction, $G(x)$ is a trigonometric and polynomial function.

For simplified analysis, form factor and structure factor can be divided by

1. Form factor: concentrated system, where inter-molecular interactions are strong;
2. Structure factor: diluted system, where inter-molecular interactions are week.

## 4.2. **GIWAXS Testing procedure**

The GIWAXS test was done in BNL CMS-11 beamline on July 14th-17th, , 2017. After freestanding samples on a silicon wafer was prepared, it was placed in a testing cell with Kapton tapes on both sides. This additional cell is used to control the humidity of the testing environment. A humidity controller and a detector are connected to the cell.

Close the cell with a Allen key. Then put the cell in CMS-17 chamber. This beam line is controlled by a python console and LabVIEW front panel.

A LabVIEW button was used to start pumping the chamber to vacuum. The python console was used to calibrate sample position after starting the beam. Subsequently, 2D scattering patterns were collected at different positions on the sample. For each point, it was tested with multiple incident angles and various humidity points.

A 2D scattering image of polyamide layer captured by GIWAXS system, as shown in Figure 11. The sample is a polysulfone membrane placed on a silicon wafer. The left down side is close to the beam center, which is calibrated using AgBH sample. Two window effects can be observed on this image, the smaller one is caused by the left Kapton window and the larger one is caused by right Kapton window. Later in the integrated radius file, the intensity were

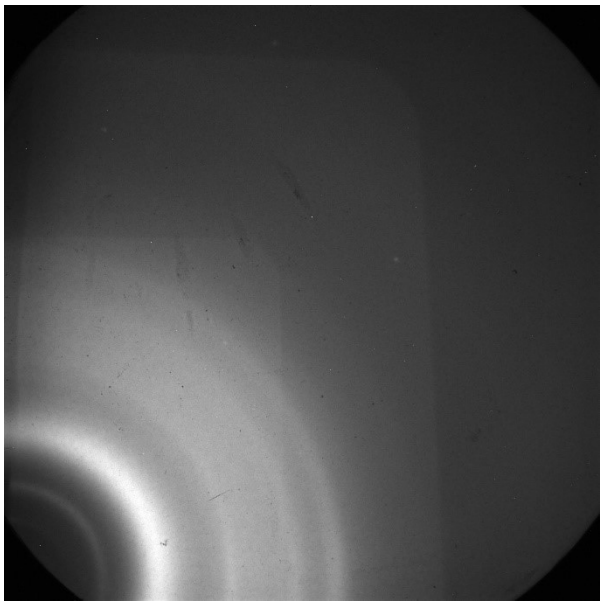

Figure 11 2D scattering image of polyamide layer captured by GIWAXS system.

normalized by these two window peaks.

### 4.3. **GIWAXS Data analysis**

GIWAXS Data analysis has been carried out with python programming. First a calibration line is applied by a AgBH sample to calibrate the $Q_Z$ profile. Then the radius profile of 2D images is integrated. In our research, to reduce defect, the image with only 0-30° angle was integrated.

Some of the interesting comparison was shown below.

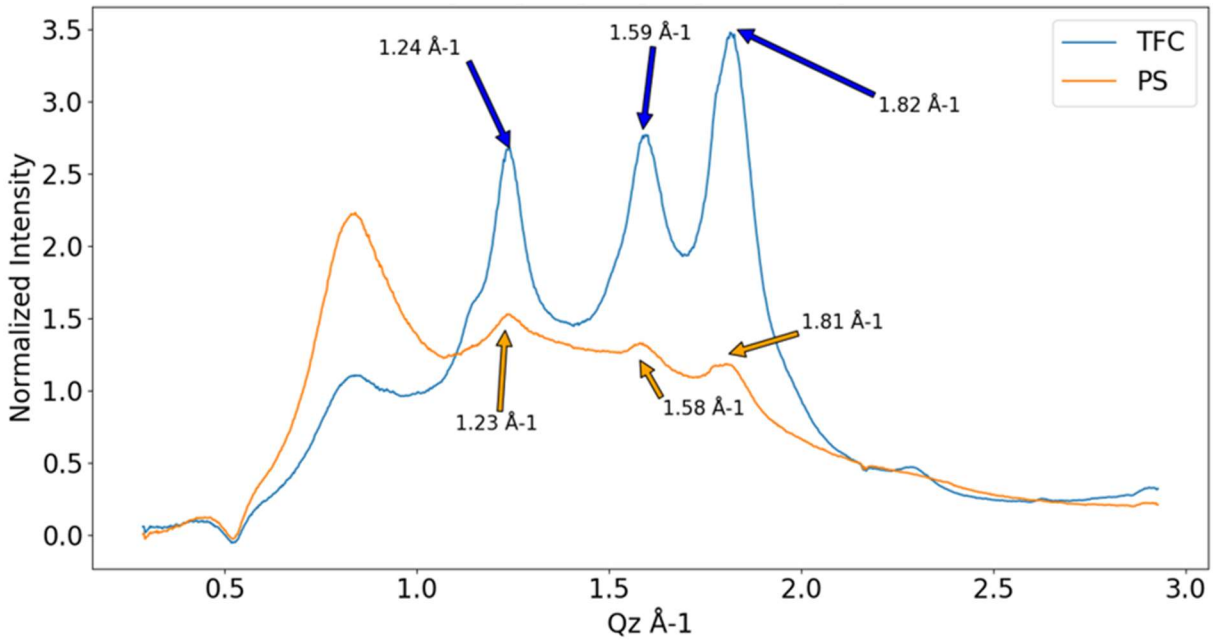


Figure 12 GIWAXS comparison of TFC membrane to PS membrane.

1. Polysulfone substrate compared with polyamide on polysulfone (TFC membrane)

These 2 curves are background-subtracted at the same incident angle 0.15°. The left two peaks positions are less than 1.0 Å $^{-1}$ and are assigned to the refraction of Kapton tapes on side of the cell. So, these two peaks can be used to normalize all the intensity of profiles. TFC membrane has 3 peaks at 1.24, 1.58 and 1.82 Å $^{-1}$ and PS membrane has 3 peaks at 1.23, 1.58 and 1.81 Å $^{-1}$. These peak positions are similar but the intensities are different. For these peaks, the corresponding characteristic real space distances are 5.1 Å, 4.0 Å and 3.5 Å. 5.1 Å is in accordance with previous literature which shows the average molecular spacing is 5.2 Å-5.3 Å [16]. This molecular spacing is less than salt ion size (~ 1nm) so that can explain why polyamide layer can filter out salt. 4.0 Å and 3.5 Å was unexplained before, they might come from the

structure factor of the polyamide layer. With PA layer on top of the substrate, this high $Q_Z$ value are greatly increased, which indicates a dense core layer is formed on top of the substrate.

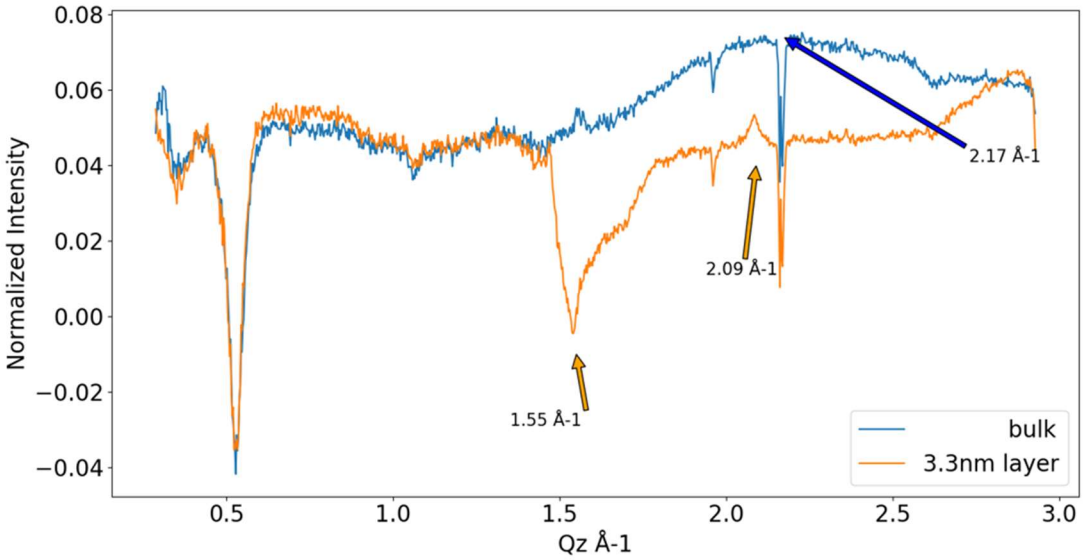


Figure 13 GIWAXS comparison of bulk film to thin film of 3.3 nm.

2. bulk material vs thin film.

At lower Qz (<1.4 Å $^{-1}$), these two peaks are identical, which indicates bulk layer and thin layer are similar at the inter-molecular scale. However, at larger $Q_Z$ the bulk film continues to go up and has a smooth peak at 2.23 Å $^{-1}$ (2.82 Å in real space) The thin film goes down dramatically at 1.55 Å $^{-1}$ (4.01 Å in real space), and then back up to reach a peak at 2.10 Å $^{-1}$. The bulk layer behaves smooth and continuous, while thin layer has dramatic peaks. One major problem in this image is the noise is strong so that both curves are turbulent. That is coming from the additional cell we added to the chamber to control humidity. This problem can be solved by simply placing the samples in vacuum as a comparison.

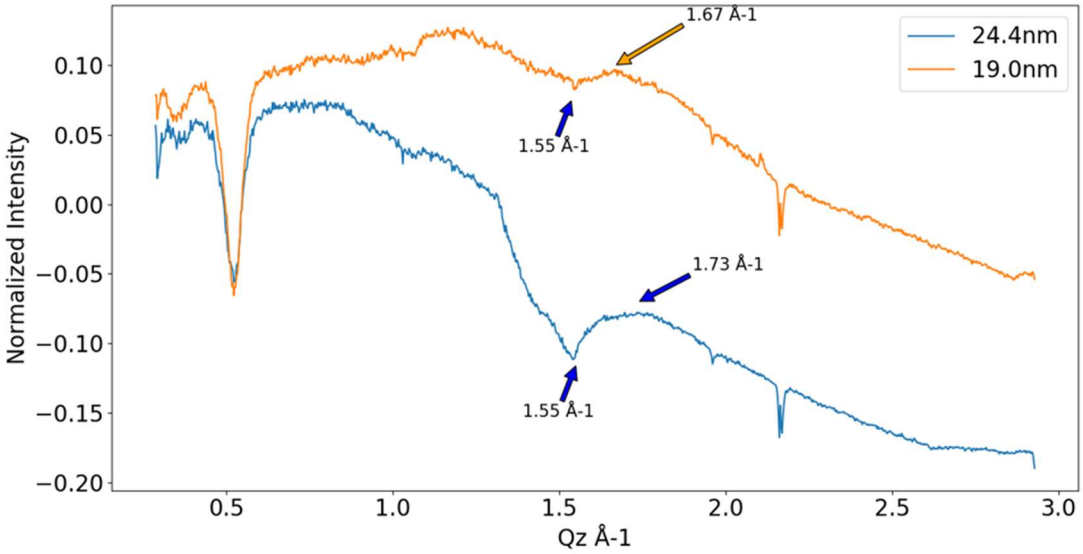


Figure 14 GIWAXS comparison of 2 similar layer with slightly different thickness.

3. Comparison of 2 similar layer with slightly different thickness

Two curves are similar in shape which indicates their structural factor are similar. Both peaks go down at 1.55 $Å^{-1}$ (4.01 Å in real space). But 19.0 nm layer goes up at 1.67 $Å^{-1}$ (3.76 Å in real space) and 24.4 nm layer goes up at 1.73$Å^{-1}$ (3.63 Å in real space). That means the inter-molecular spacing in 24.4 nm layer is less than that of 19.9 nm. That's because layer corresponding to 24.4 nm is formed by higher concentration of monomers and unreacted monomers stuck in the layer is further cross-linked after the layer formed.

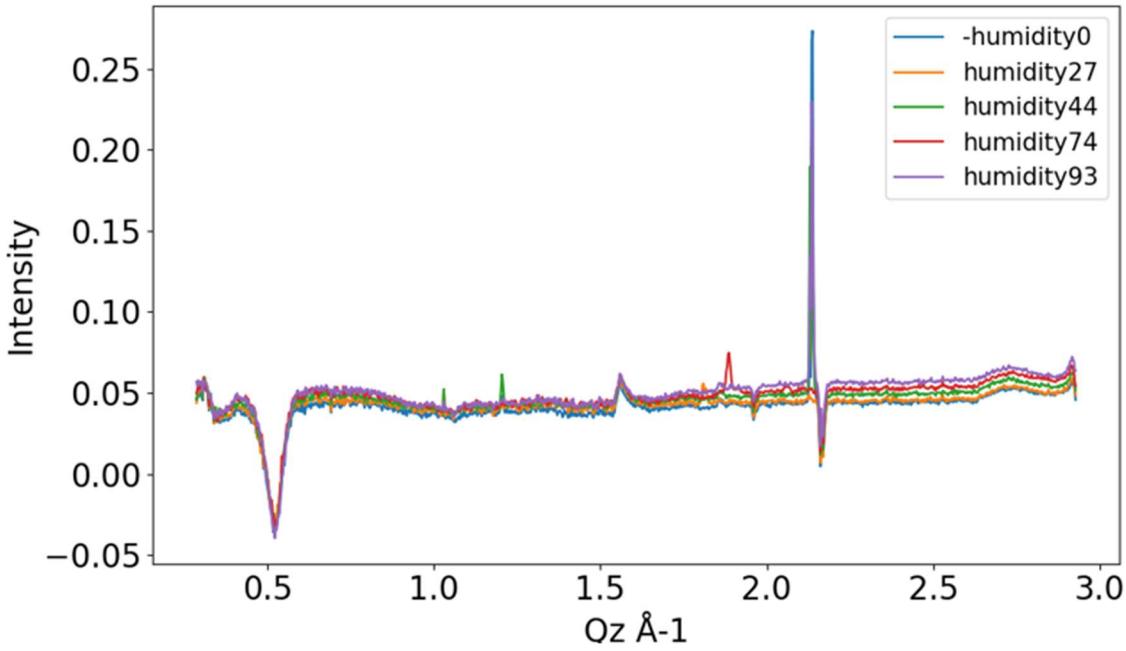


Figure 15 These 2 curves are background-reduced at the same incident angle 0.15°.

4. Humidity comparison

These are the same layer (MPD0.01 wt%, TMC 0.0005 wt%, 5.3 nm) scattering result of 5 humidity points, and they are almost identical. This indicates that polyamide layer is robust in humid environment. Also this result is in contrast with literature[39]. The difference is, their sample is made layer-by-layer using spin-coating, while my sample is made one-time at liquid interface. That means the layer thickness change in the layer-by-layer sample is coming from the layer gap instead of within the polyamide structure.

## 4.4. **GIWAXS test summary**

GIWAXS was used to study intra-molecular structure of polyamide layer. The results showed:

1. Average molecular spacing for polyamide layer is 5.1 Å, which is in accordance with literature.
2. Monomer concentration has large effects on polyamide layer structure factor. Shift of scattering peaks are observed, while the form factor at low Q is identical.
3. Humidity level does not strongly affect polyamide layer structure.

Also, some improvements can be made in my current GIWAXS test includes

1. The background noise is not completely removed. Next time, I plan to do GIWAXS test in vacuum first to reduce background noise.
2. Develop an advanced scattering model to fit data.
3. Reflectometry result at multiple humidity points should be done to compare with GIWAXS result; AFM test of ultra-thin layer should be conducted as comparison.

# Chapter 5. **High pressure desalination test**

RO membranes are tested under 800 psi with 3.5 wt% salt. [38], [40]. A high-pressure desalination system is built with 6 testing cells, as shown in Figure 16.

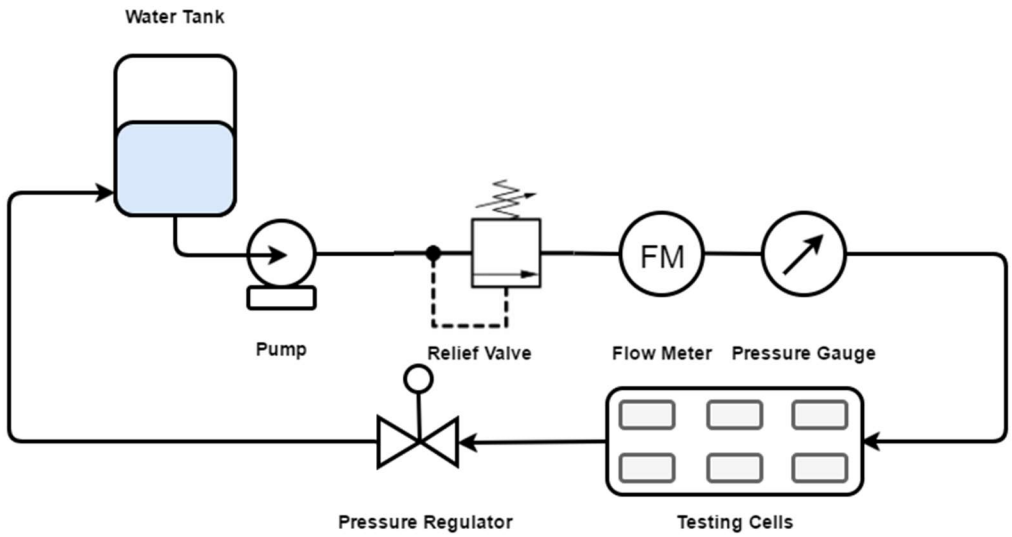


Figure 16 High-pressure desalination system. This system can run at 1000psi, the maximum flow rate can go up to 3 GPM, therefore, can run RO test at 800 psi as standard pressure. The system has 6 testing cells of 1.5×3.5 inch membrane.

## 5.1. **RO membrane preparation procedure**

The fabrication of polyamide layer on polysulfone substrate is described as follows: 2 wt% MPD water solution and TMC 0.1 wt% hexane solution weres prepared. First soaking the polysulfone substrate (6 × 6 inches) in MPD solution for 2 min, and then, take out the polysulfone substrate onto a glass plate. The excess MPD solution on polysulfone was removed with a glass rod followed by taping the substrate on the glass plate. Next step, 6 g of TMC is delivered on the polysulfone substrate, and remained for 20 sec before drained out. The

membrane was then heatedat 120 ºC for 20 min. The TFC membrane was stored in water and was ready to be used.

## 5.2. **High pressure desalination system testing procedure**

The testing procedure is as follows. First RO membranes as prepared or commercial desalination membranes were cut into 1.5 × 3.5 inches coupons and placed in all 6 cells. After cells were closed, the by-pass valve and 2 switches control the flow rate to the cells was completely turned on before the power starts. Then, started the pump and slowly turned off the by-pass valve, and the pressure will increase to 40 psi. The back pressure regulator is then regulated to achieve the desired pressureto adjust the flow rate. Usually the samples were tested to 800 psi and 2 GPM (1 GPM for individual cell). And a cooling system was used to keep the water temperature of 25 °C during the test.

## 5.3. **Desalination result and discussion**

Table 1 High-pressure desalination Result

| Membrane types | Rejection rate | Flux (L/(hr·m$^2$)) |
|---|---|---|
| SW30XLE (commercial) | 99.4% | 18 |
| SW30HR (commercial) | 99.5% | 15 |
| VTC-82V(commercial) | 99.3% | 26 |
| Polyamide on polysulfone | 98.1% | 22 |

Table 1 shows desalination testing result for 3 commercial membranes and the polyamide membrane on polysulfone substrate. Three types of RO commercial membrane were compared with the RO membrane based on polysulfone substrate. The rejection rate 98.1% of the polyamide membrane base do PS35 substrate, which was comparable to that of commercially available ones (over 99.3%); and the flux was also about the same. The concentration of monomers used are 2 wt% (MPD) and 0.1 wt% (TMC), respectively, where the thickness estimated as 100 nm and the surface, as expected, crumpled.

## 5.4. **Polyamide layer on-substrate characterization**

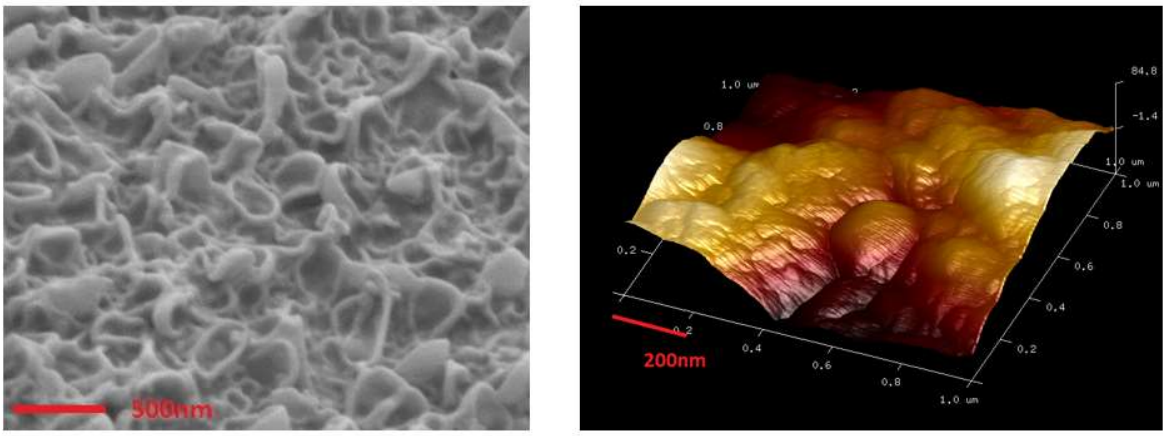


Figure 17 Left: SEM top view of polyamide layer on polysulfone membrane. Monomer concentration: MPD 2 wt%, TMC 0.1 wt%.

In Figure 17, The top structure created by high concentration TMC/MPD is crumpled and intertwined, which is in accordance with previous report. Also, the top layer covers the substrate well. Right: AFM image of the same sample. The roughness is estimated to be is 28.9 nm in 1x1 μm2 scale ased on the analysis of AFM images.

In Figure 18, SEM cross-section view of polyamide layer on two different substrates were made. For both images, the polyamide layer thickness is estimated to be 100 nm. Monomer concentration are: MPD 2 wt% TMC 0.1 wt%. The surface layer is well attached to the

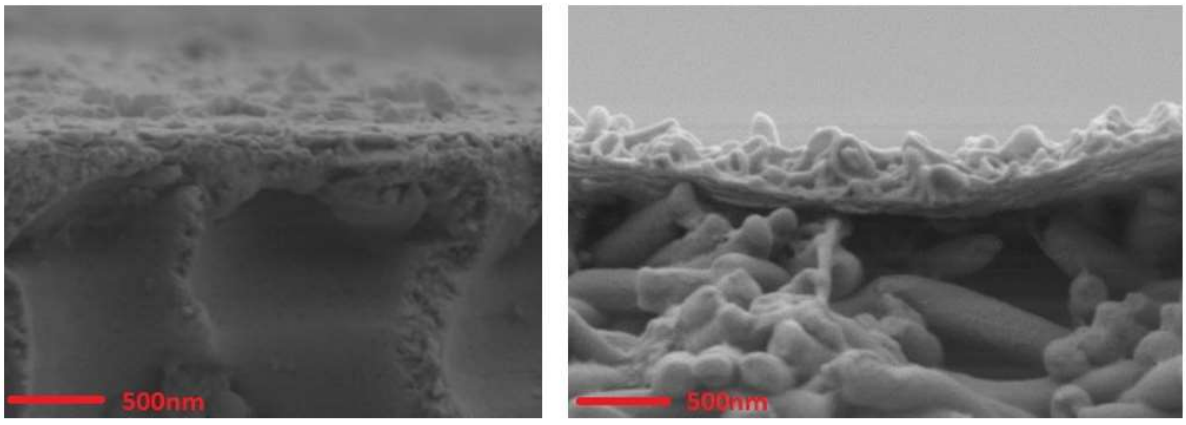


Figure 18 SEM cross-section view of polyamide layer on Left: PAN 400 and Right: Thin film nano-composite substrate.

polysulfone substrate.

## Conclusions

Research conclusion is summarized as follows.

1. Freestanding polyamide layer by interfacial polymerization was successfully made. A syringe pump-setup was used to stabilize the reaction. The layer thickness is as thin as 3.3 nm with roughness of 10 Å.
2. Reflectometry test was conducted on the freestanding sample, and a well-defined fitting model was developed. With the fitting result, the electron density of polyamide layer was figured out as close to water.
3. GIWAXS test was conducted on freestanding sample after reflectometry measurement. Average molecular spacing peak of polyamide film is 5.1 Å which is close to previously reported 5.2 Å-5.3 Å. Also, the shift of peak with layer thickness change was observed.
4. Desalination test was conducted to link filtration performance to the polyamide structure, which showed the performance of high concentration formed membrane with crumpled surface (confirmed under SEM) is comparable to commercial membrane.

My future plans include:

1. Advanced analysis of GIWAXS data and try to explain physical parameters such as porosity, water path and molecular orientation in data analysis.
2. A simulation of interfacial polymerization process that can explain crumpled surface at high monomer concentrations.

**Reference**


[1] L. F. Greenlee, D. F. Lawler, B. D. Freeman, B. Marrot, and P. Moulin, "Reverse osmosis desalination: Water sources, technology, and today's challenges," *Water Res.*, vol. 43, no. 9, pp. 2317–2348, 2009.

[2] W. J. Lau, A. F. Ismail, N. Misdan, and M. A. Kassim, "A recent progress in thin film composite membrane: A review," *Desalination*, vol. 287, pp. 190–199, 2012.

[3] X. Wang, D. Fang, B. S. Hsiao, and B. Chu, "Nanofiltration membranes based on thin-film nanofibrous composites," *J. Memb. Sci.*, vol. 469, pp. 188–197, 2014.

[4] M. L. Lind, A. K. Ghosh, A. Jawor, X. Huang, W. Hou, Y. Yang, and E. M. V Hoek, "Influence of zeolite crystal size on zeolite-polyamide thin film nanocomposite membranes," *Langmuir*, vol. 25, no. 17, pp. 10139–10145, 2009.

[5] Y. Mansourpanah, S. S. Madaeni, and A. Rahimpour, "Fabrication and development of interfacial polymerized thin-film composite nanofiltration membrane using different surfactants in organic phase; study of morphology and performance," *J. Memb. Sci.*, vol. 343, no. 1–2, pp. 219–228, 2009.

[6] B. H. Jeong, E. M. V Hoek, Y. Yan, A. Subramani, X. Huang, G. Hurwitz, A. K. Ghosh, and A. Jawor, "Interfacial polymerization of thin film nanocomposites: A new concept for reverse osmosis membranes," *J. Memb. Sci.*, vol. 294, no. 1–2, pp. 1–7, 2007.

[7] V. Freger, "Nanoscale heterogeneity of polyamide membranes formed by interfacial polymerization," *Langmuir*, vol. 19, no. 11, pp. 4791–4797, 2003.

[8] Y. Zhao, C. Qiu, X. Li, A. Vararattanavech, W. Shen, J. Torres, C. Hélix-Nielsen, R. Wang, X. Hu, A. G. Fane, and C. Y. Tang, "Synthesis of robust and high-performance aquaporin-based biomimetic membranes by interfacial polymerization-membrane preparation and RO performance characterization," *J. Memb. Sci.*, vol. 423–424, pp. 422–428, 2012.

[9] B. Mi, O. Coronell, B. J. Mariñas, F. Watanabe, D. G. Cahill, and I. Petrov, "Physico-chemical characterization of NF/RO membrane active layers by Rutherford backscattering spectrometry," *J. Memb. Sci.*, vol. 282, no. 1–2, pp. 71–81, 2006.

[10] R. J. Petersen, "Composite reverse osmosis and nanofiltration membranes," *J. Memb. Sci.*, vol. 83, no. 1, pp. 81–150, 1993.

[11] N. Misdan, W. J. Lau, and A. F. Ismail, "Seawater Reverse Osmosis (SWRO) desalination by thin-film composite membrane—Current development, challenges and future prospects," *Desalination*, vol. 287, pp. 228–237, 2012.

[12] S. H. Kim, S. Y. Kwak, B. H. Sohn, and T. H. Park, "Design of TiO2 nanoparticle self-assembled aromatic polyamide thin-film-composite (TFC) membrane as an approach to solve biofouling problem," *J. Memb. Sci.*, vol. 211, no. 1, pp. 157–165, 2003.

[13] W. A. Phillip, J. D. Schiffman, and M. Elimelech, "High Performance Thin-Film

Membrane," vol. 44, no. 10, pp. 3812–3818, 2010.

[14] S. Karan, Z. Jiang, and A. G. Livingston, "Sub–10 nm polyamide nanofilms with ultrafast solvent transport for molecular separation," *Science (80-. ).*, vol. 348, no. 6241, pp. 1347–1351, 2015.

[15] T. Matthews, "Growth Dynamics, Charge Density, and Structure of Polyamide Thin-Film Composite Membranes," 2014.

[16] P. S. Singh, P. Ray, Z. Xie, and M. Hoang, "Synchrotron SAXS to probe cross-linked network of polyamide 'reverse osmosis' and 'nanofiltration' membranes," *J. Memb. Sci.*, vol. 421–422, pp. 51–59, 2012.

[17] C. M. Sorensen and G. M. Wang, "Size distribution effect on the power law regime of the structure factor of fractal aggregates," *Phys. Rev. E*, vol. 60, no. 6, p. 7143, 1999.

[18] H. D. Bale and P. W. Schmidt, "Small-angle X-ray-scattering investigation of submicroscopic porosity with fractal properties," *Phys. Rev. Lett.*, vol. 53, no. 6, p. 596, 1984.

[19] L. A. Feigin, D. I. Svergun, and others, *Structure analysis by small-angle X-ray and neutron scattering*. Springer, 1987.

[20] R. Oizerovich-Honig, V. Raim, and S. Srebnik, "Simulation of thin film membranes formed by interfacial polymerization," *Langmuir*, vol. 26, no. 1, pp. 299–306, 2010.

[21] P. Meakin, T. Vicsek, and F. Family, "Dynamic cluster-size distribution in cluster-cluster aggregation: Effects of cluster diffusivity," *Phys. Rev. B*, vol. 31, no. 1, pp. 564–569, 1985.

[22] P. Meakin and J. M. Deutch, "Monte Carlo simulation of diffusion controlled colloid growth rates in two and three dimensions," *J. Chem. Phys.*, vol. 80, no. 5, p. 2115, 1984.

[23] P. Meakin and Z. B. Djordjevic, "Cluster-cluster aggregation in two-monomer systems," *J. Phys. A. Math. Gen.*, vol. 19, no. 11, p. 2137, 1986.

[24] J. Ji and M. Mehta, "Mathematical model for the formation of thin-film composite hollow fiber and tubular membranes by interfacial polymerization," *J. Memb. Sci.*, vol. 192, no. 1–2, pp. 41–54, 2000.

[25] Y. Huang and D. R. Paul, "Effect of MolecularWeight and Temperature on Physical Aging of ThinGlassy Poly(2,6-dimethyl-1,4-phenylene oxide) Films," *J. Polym. Sci. Part B Polym. Phys.*, vol. 45, no. April, pp. 1390–1398, 2007.

[26] A. Moldovan, F. Feldmann, G. Krugel, M. Zimmer, J. Rentsch, M. Hermle, A. Roth-Fölsch, K. Kaufmann, and C. Hagendorf, "Simple cleaning and conditioning of silicon surfaces with UV/ozone Sources," *Energy Procedia*, vol. 55, pp. 834–844, 2014.

[27] U. Irvine, "Cleaning Procedures for Silicon Wafers," *Fabrication*, no. Di, pp. 2–5, 2010.

[28] Y. Song, P. Sun, L. L. Henry, and B. Sun, "Mechanisms of structure and performance controlled thin film composite membrane formation via interfacial polymerization process," *J. Memb. Sci.*, vol. 251, no. 1–2, pp. 67–79, 2005.

[29] J. T. Fraval and M. T. Godfrey, “(12) UnIted States Patent,” vol. 1, no. 12, p. 5, 2002.

[30] R. J. King and S. P. Talim, “A Comparison of Thin Film Measurement by Guided Waves, Ellipsometry and Reflectometry,” *Opt. Acta Int. J. Opt.*, vol. 28, no. 8, pp. 1107–1123, 1981.

[31] A. K. Ghosh, B. H. Jeong, X. Huang, and E. M. V Hoek, “Impacts of reaction and curing conditions on polyamide composite reverse osmosis membrane properties,” *J. Memb. Sci.*, vol. 311, no. 1–2, pp. 34–45, 2008.

[32] B. M. Ocko, “Chem 157: Lecture 17 (X-ray reflectivity),” vol. 17.

[33] W. Incident, “Main Notation Used in This Book,” pp. 343–348.

[34] L. van Hove, “Correlations in Space and Time and Born Approximation in Systems of Interacting Particles,” *Physical Review*, vol. 93, no. 1. pp. 249–262, 1954.

[35] Z. Jiang, “Theory of GISAXS,” *Am. Crystallogr. Assoc. Meet.*, 2014.

[36] P. Vachette, “Scattering of X-rays,” *EMBO Pract. Course Solut. Scatt. from Biol. Macromol.*, 2010.

[37] J. Perlich, J. Rubeck, S. Botta, R. Gehrke, S. V. Roth, M. A. Ruderer, S. M. Prams, M. Rawolle, Q. Zhong, V. K??rstgens, and P. M??ller-Buschbaum, “Grazing incidence wide angle x-ray scattering at the wiggler beamline BW4 of HASYLAB,” *Rev. Sci. Instrum.*, vol. 81, no. 10, pp. 1–7, 2010.

[38] A. Vrij, “Mixtures of hard spheres in the Percus–Yevick approximation. Light scattering at finite angles,” *J. Chem. Phys.*, vol. 71, no. 8, pp. 3267–3270, 1979.

[39] E. P. Chan, A. P. Young, J. H. Lee, and C. M. Stafford, “Swelling of ultrathin molecular layer-by-layer polyamide water desalination membranes,” *J. Polym. Sci. Part B Polym. Phys.*, vol. 51, no. 22, pp. 1647–1655, 2013.

[40] M. Kurihara, H. Yamamura, and T. Nakanishi, “High recovery/high pressure membranes for brine conversion SWRO process development and its performance data,” *Desalination*, vol. 125, no. 1–3, pp. 9–15, 1999.